



T2R bitter taste receptors regulate apoptosis and may be associated with survival in head and neck squamous cell carcinoma

Ryan M. Carey¹ , Derek B. McMahon¹, Zoey A. Miller¹, TaeBeom Kim², Karthik Rajasekaran¹, Indiwari Gopallawa¹, Jason G. Newman¹, Devraj Basu¹, Kevin T. Nead^{2,3}, Elizabeth A. White¹ and Robert J. Lee^{1,4} 

1 Department of Otorhinolaryngology, University of Pennsylvania Perelman School of Medicine, Philadelphia, PA, USA

2 Department of Epidemiology, Division of Cancer Prevention and Population Sciences, The University of Texas MD Anderson Cancer Center, Houston, TX, USA

3 Department of Radiation Oncology, The University of Texas MD Anderson Cancer Center, Houston, TX, USA

4 Department of Physiology, University of Pennsylvania Perelman School of Medicine, Philadelphia, PA, USA

Keywords

apoptosis; calcium; cell signaling; genetics; head and neck squamous cell carcinoma; taste receptors

Correspondence

R. M. Carey and R. J. Lee, Department of Otorhinolaryngology—Head and Neck Surgery, Hospital of the University of Pennsylvania, 3400 Spruce Street, 5th floor Ravdin Suite A, Philadelphia, PA 19104, USA
Tel: +215 573 9766
E-mail: ryan.carey@pennmedicine.upenn.edu (R.M.C.); rjl@pennmedicine.upenn.edu (R.J.L.)

(Received 3 June 2021, revised 16 September 2021, accepted 28 October 2021, available online 14 December 2021)

doi:10.1002/1878-0261.13131

Better management of head and neck squamous cell carcinomas (HNSCCs) requires a clearer understanding of tumor biology and disease risk. Bitter taste receptors (T2Rs) have been studied in several cancers, including thyroid, salivary, and GI, but their role in HNSCC has not been explored. We found that HNSCC patient samples and cell lines expressed functional T2Rs on both the cell and nuclear membranes. Bitter compounds, including bacterial metabolites, activated T2R-mediated nuclear Ca^{2+} responses leading to mitochondrial depolarization, caspase activation, and ultimately apoptosis. Buffering nuclear Ca^{2+} elevation blocked caspase activation. Furthermore, increased expression of T2Rs in HNSCCs from The Cancer Genome Atlas is associated with improved overall survival. This work suggests that T2Rs are potential biomarkers to predict outcomes and guide treatment selection, may be leveraged as therapeutic targets to stimulate tumor apoptosis, and may mediate tumor-microbiome crosstalk in HNSCC.

1. Introduction

Head and neck squamous cell carcinoma (HNSCC) is the 6th most common cancer worldwide, with an

expected 30% incidence increase by 2030 [1]. HNSCC often presents with locally advanced disease [2], and approximately half of patients die ≤ 5 years after diagnosis [3]. Treatment is based on clinical and pathologic

Abbreviations

3-oxo-C12HSL, N-3-oxo-dodecanoyl-L-homoserine lactone; Ca^{2+} , calcium; Ca^{2+}_i , intracellular calcium; Ca^{2+}_{nuc} , nuclear calcium; eCFP, enhanced cyan fluorescent protein; ER, endoplasmic reticulum; FRET, Förster resonance energy transfer; GFP, G protein-coupled receptors; HNSCC, head and neck squamous cell carcinoma; HPV, human papillomavirus; HPV⁻, human papillomavirus negative; HPV⁺, human papillomavirus positive; IP₃, inositol trisphosphate; IP₃R, inositol trisphosphate receptor; NO, nitric oxide; PLC, phospholipase C; PQS, *Pseudomonas* quinolone signal; PTC, phenylthiocarbamide; qPCR, quantitative reverse transcription PCR; R-GECO-nls, nuclear-localized genetically encoded calcium biosensor; T2R, bitter taste receptor protein; *TAS2R*, bitter taste receptor gene; TCGA, The Cancer Genome Atlas; TMRE, tetramethylrhodamine ethyl ester; $\Delta\Psi_m$, mitochondrial membrane potential.

risk factors, typically consisting of a combination of surgery, radiation, chemotherapy, and immunotherapy in select cases [4,5]. Because treatment side effects impact quality of life, it is important to tailor the aggressiveness of therapy to disease risk [6].

HNSCCs associated with human papillomavirus (HPV) show improved overall survival and recurrence-free survival compared with HPV-negative tumors. Thus, HPV status is an important tool for risk stratification and treatment selection [7,8]. There is need for additional methods or biomarkers for stratifying disease risk. There is also a need for alternative therapies that maximize survival while minimizing morbidity in HNSCC. The ideal cancer therapy may be one that exploits cellular machinery to prevent immune system evasion or impact tumor microenvironment.

The current study suggests that bitter taste receptors (T2Rs) may be important for risk stratification and/or as novel therapeutic targets in HNSCC. Initially identified on the tongue, T2Rs are expressed in other tissues, including the gastrointestinal [9] and airway epithelia [10,11]. There are 25 human T2R isoforms [10] encoded by bitter taste receptor gene (*TAS2R*) genes [12]. T2Rs are G protein-coupled receptors (GPCRs) that signal through $G\alpha$ -mediated cAMP decrease and $G\beta\gamma$ activation of phospholipase C (PLC) and calcium (Ca^{2+}) release [10]. T2Rs serve a diverse array of chemosensory functions, including in innate immunity [10,13]. For example, T2Rs in nasal cells bind bacterial products to activate Ca^{2+} -driven nitric oxide (NO) production to increase cilia beating and kill bacteria [10,11].

T2Rs have also been explored in some cancers [14–23], including thyroid [17], salivary [18], and gastrointestinal cancers [14–16,19,22,23]. Polymorphisms in the *TA2R38* gene encoding the T2R38 receptor are associated with elevated cancer risk [15,16,23,24]. Individuals with specific *TAS2R3* and 4 haplotypes may have lower risk of papillary thyroid cancer [17]. Recent work demonstrated elevated expression of many GPCRs in solid tumors compared with normal tissue [25]. While there is prior work on T2Rs in cancer, an association between T2Rs and HNSCC and the potential T2R signaling pathways within cancer cells are unknown.

We hypothesized that HNSCCs may differentially express *TAS2Rs* compared with normal tissue and some T2Rs are functional and regulate cellular processes. We characterized *TAS2R* expression in HNSCC patient samples and cell lines. We demonstrate that some T2Rs have intracellular or intranuclear localization and can be activated to cause mitochondrial

depolarization and apoptosis in HNSCC cells. We subsequently evaluated HNSCC patients for association of *TAS2R* expression levels with survival outcomes using The Cancer Genome Atlas (TCGA).

2. Materials and methods

Unless noted, all reagents and protocols were used as previously described [11,26–29]. All reagents and catalogue numbers are in Table S1.

2.1. Cell culture

SCC4, SCC15, SCC90, and SCC152 cells were from ATCC (Manassas, VA USA). UMSCC47 (SCC47) was from Sigma-Aldrich (St. Louis, MO USA). OCTT2 cell line was derived from a surgical specimen of an oral SCC tumor [30]. VU147T was from Dr. Hans Joenje, VU Medical Center, the Netherlands. All cancer cell lines were grown in submersion in high glucose Dulbecco's modified Eagle medium (Gibco; Gaithersburg, MD, USA) plus 10% FBS, penicillin/streptomycin mix (Gibco), and nonessential amino acids (Gibco). Primary gingival keratinocytes were from ATCC (Manassas, VA, USA) and used within 2 passages using dermal cell basal keratinocyte medium (ATCC).

2.2. Patient samples

This study was approved by the University of Pennsylvania Institutional Review Board (protocol #417200). All subjects provided written informed consent for study participation. SCC specimens were obtained from patients undergoing diagnostic biopsies of HNSCC tumors as part of routine clinical care. Tissue acquisition was done in accordance with the University of Pennsylvania guidelines for the use of residual clinical material and in accordance with the U.S. Department of Health and Human Services code of federal regulation Title 45 CFR 46.116 and the Declaration of Helsinki. Tumor and contralateral normal tissue was obtained. Specimens were divided for pathologic evaluation, and expression analysis samples were collected in TRIzol (Thermo Fisher Scientific).

All tumor specimens had final pathology consistent with SCC. HPV positivity was determined after p16 testing, based on immunohistochemistry that demonstrated $\geq 70\%$ of tumor nuclear and cytoplasmic staining [31]. Testing was performed on cancers of the oropharynx, but not for cancers of other HNSCC sites per the University of Pennsylvania guidelines.

2.3. Quantitative reverse transcription PCR

Patient samples and subconfluent cultures were resuspended in TRIzol (Thermo Fisher Scientific). RNA was isolated and purified (Direct-zol RNA kit; Zymo Research), reverse transcribed via High-Capacity cDNA Reverse Transcription Kit (Thermo Fisher Scientific), and quantified using TaqMan qPCR probes for the 25 *TAS2R* genes and UBC (QuantStudio 5; Thermo Fisher Scientific). The expression of each *TAS2R* gene was normalized to housekeeping UBC gene, which has been shown to be a stable housekeeping gene in many cancer cell lines [32,33].

2.4. Live cell imaging

Cells were loaded with 5 μM of Fluo-4-AM or Fluo-8-AM for 45 min at room temperature in the dark, then imaged using an Olympus IX-83 microscope (20x 0.75 NA PlanApo objective), FITC filters, Orca Flash 4.0 sCMOS camera (Hamamatsu, Tokyo, Japan), MetaFluor (Molecular Devices, Sunnyvale, CA USA), and XCite 120 LED Boost (Excelitas Technologies). For nuclear Ca^{2+} , R-GECO-nls [34] was transfected using Lipofectamine 3000 (Thermo Fisher Scientific) 24–48 h prior to imaging. Live cell images were taken as above with standard TRITC filters.

For Flip-GFP, cells were transfected and imaging was carried out on an Olympus IX-83 microscope as above with 10x (0.4 NA) or 4x (0.16 NA) objective and FITC and TRITC filter sets. For CFP-DEVD-mVenus, cells were imaged at 40x (0.75NA objective) with CFP/YFP filters (Chroma 89002-ET-ECFP/EYFP) in excitation and emission filter wheels (Sutter Lambda LS). Images were acquired at 37 °C using a stage-top incubator (Tokai Hit, Tokyo, Japan).

2.5. Immunofluorescence

Cultures were fixed in 4% paraformaldehyde for 20 min at room temperature, followed by blocking and permeabilization in DPBS containing 5% normal donkey serum, 1% BSA, 0.2% saponin, and 0.1% Triton X-100 for 45 min. Cultures were with T2R or tubulin antibodies (1:100) at 4 °C overnight. Several T2R antibodies (T2R14, T2R4) were validated previously [11,13,35]. Cultures were then incubated with AlexaFluor-labeled donkey secondary antibodies (1:1000) at 4 °C for 1 h and then mounted with Fluoroshield with DAPI (Abcam, Cambridge, UK). Images were obtained using an Olympus IX-83 microscope (60x 1.4 NA oil; METAMORPH software, San Jose, CA, USA).

2.6. Mitochondrial membrane potential and apoptosis measurements

JC-1 dye was added to subconfluent cells on 24-well glass-bottom plates (CellVis, Mountain View, CA, USA) 10 min prior to measurements (ex.488/em.535 and em.590). CellEvent Caspase 3/7 was added directly prior to measurements (ex.495/em.540) per manufacturer's specifications. XTT was added directly prior to measurements at 475 and 660 nm. All data for JC-1, CellEvent Caspase 3/7, and XTT assays were obtained Tecan (Männedorf, Switzerland) Spark 10M. TMRE, Red Dot 2, and Hoechst were added per manufacturer's specifications. Data were obtained using an Olympus IX-83 microscope (20x 0.8 NA objective; MetaFluor, MetaMorph, San Jose, CA, USA) with DAPI, TRITC, and Cy5 filters.

2.7. The Cancer Genome Atlas analysis

Data were obtained from the PanCancer Atlas and Firehose Legacy datasets of TCGA from cBio Cancer Genomics Portal (cbioportal.org) [36,37]. The PanCancer Atlas dataset was used for comparisons of *TAS2R* mRNA expression in tumor and adjacent normal tissue. These data were derived from the relative expression of a gene in a tumor sample compared with the expression distribution of all adjacent normal tissue samples in the cohort. The data were provided as an expression z-score which is the number of standard deviations away from the mean of expression in the normal tissue reference population. The tumor-normal expression analysis was conducted by selecting tumors with ICD codes corresponding to the anatomic sites of oropharynx (C09.9, C01.9, C10.9) and oral cavity (C02.9, C04.9, C06.0, C03.9, C00.9, C14.8). Tumors were further stratified by HPV status based on expression of viral E6/E7 as previously described [38]. The database was queried for all detectable *TAS2R* genes.

The larger Firehose Legacy dataset was used for all other TCGA analyses of *TAS2Rs*. We included all HNSCC samples with mutation and copy number alteration data available. Expression comparisons were based on each queried gene compared with that gene's expression in a reference population consisting of all samples that are diploid for the gene [37].

2.8. Data analysis and statistics

t-Tests (two comparisons only) and one-way ANOVA (>2 comparisons) were calculated using GRAPHPAD PRISM (San Diego, CA, USA) with appropriate posttests, as indicated. Additional data analysis was

performed using the cBio PORTAL software, Microsoft Excel, or R version 4.0.3 (2020-10-10). All figures used the following annotations: $P < 0.05$ (*), $P < 0.01$ (**), $P < 0.001$ (***), and no statistical significance (ns). All data points represent the mean \pm SEM.

3. Results

3.1. T2Rs are differentially expressed and localized in HNSCC

We examined expression of 25 *TAS2Rs* in HNSCC tissue from patients undergoing diagnostic biopsies during routine clinical care. Tissue was obtained from the tumor site and corresponding contralateral normal site from 10 patients (Table S2). Quantitative reverse transcription PCR (qPCR) demonstrated variable expression of *TAS2Rs* (Fig. 1A,B). In aggregate, there were no significant differences in expression of individual *TAS2Rs* between control and cancer samples (Fig. 1A). However, comparison at the individual patient level demonstrated that some individuals had increased *TAS2R* expression in the tumor specimens while others had decreased expression compared with matched control tissue (Fig. 1B). This small sample size suggests that T2Rs are expressed in HNSCC tissue, but was not robust enough to determine differences in normal vs cancer tissue, including potential associations with clinical outcomes.

TAS2R expression was measured via qPCR in HNSCC cell lines SCC4, SCC15, SCC47, SCC90, SCC152, OCTT2, and VU147T (Fig. S1). Like patient samples, cells had variable *TAS2R* expression, but specific *TAS2Rs* were consistently high, including *TAS2R4*, *TAS2R14*, *TAS2R19* (also known as *TAS2R23* or *TAS2R48*), *TAS2R20* (also known as *TAS2R49*), and *TAS2R30* (formerly known as *TAS2R47*), *TAS2R43*, and *TAS2R45*. Similarities in *TAS2R* expression between cell lines and tumor specimens suggest these cells may be useful for studying T2R signaling in HNSCC. We also confirmed expression of T2R4, T2R8, T2R10, T2R30, and T2R39 in HNSCC cells by western blot (Fig. S2).

To compare our clinical samples to a larger dataset, we performed an mRNA expression analysis of TCGA for tumor and adjacent normal tissue from 390 patients with HNSCC of the oral cavity and oropharynx (Fig. 2). The *TAS2R* expression was depicted as z -scores calculated relative to normal tissue which indicates how many standard deviations away expression of the tumor tissue lie from the expression of the normal tissue. We find that *TAS2R* expression z -scores tended to be low for several isoforms including

TAS2R8, *TAS2R1*, and *TAS2R42* which were low in $\sim 90\%$ of patients. In contrast, z -scores for other *TAS2Rs* such as *TAS2R14* and *TAS2R20* were high in $\sim 20\%$ – 25% of patients. *TAS2R4* and *TAS2R19* expression z -scores were high for a smaller proportion of patients at $\sim 1\%$ and $\sim 4\%$, respectively. There were no obvious trends in expression based on anatomic site or HPV status.

Next, we used confocal immunofluorescence microscopy to visualize T2R localization. Fixed SCC47 and SCC4 cells were stained with antibodies targeting endogenous tubulin and T2Rs (Figs 3 and S3). Interestingly, T2R42 localized to the nucleus in both cell lines and T2R13 was nuclear-localized in SCC47 but not SCC4. Other T2Rs (including 4, 8, 10, 14, 30/47, and 46) appeared to localize to intracellular membranes, potentially including the endoplasmic reticulum (ER). T2R expression on the nuclear membrane is novel, and fits with our studies of airway cells, where squamous dedifferentiation promotes intracellular and even nuclear localization (preprint [39]).

3.2. T2R-activated nuclear Ca^{2+} responses in HNSCC

To determine whether T2Rs in HNSCC cells are functional, we examined agonist-induced intracellular calcium (Ca^{2+}_i) changes in SCC47, SCC4, SCC15, SCC152, SCC90, OCT22, and VU147T loaded with Ca^{2+} indicator Fluo-4 (Fig. 4A). We tested bitter compounds targeting multiple T2Rs (Fig. 4B). SCC4 and SCC47 exhibited Ca^{2+}_i elevations in response to bitter agonists denatonium benzoate, quinine, diphenidol, flufenamic acid, parthenolide, thujone, and the *P. aeruginosa* quorum-sensing molecule N-3-oxo-dodecanoyl-L-homoserine lactone (3-oxo-C12HSL, $100\ \mu\text{M}$; Figs 4A–D and S4). Similarly, SCC15, SCC152, SCC90, OCT22, and VU147T exhibited Ca^{2+}_i responses to a smaller subset of screened bitter agonists (Fig. S5). None of the cells responded to T2R38 agonist phenylthiocarbamide (PTC), consistent with *TAS2R38* expression at very low levels.

In heterologous expression studies, denatonium benzoate activates ~ 8 T2Rs (Fig. 4B) while sodium benzoate activates only T2R14 and T2R16 very weakly (mM effective concentrations) [40] (Fig. 4B). Therefore, we used sodium benzoate as a pH and osmolarity control. Denatonium benzoate activated Ca^{2+}_i responses while equimolar sodium benzoate did not (Fig. 4A,C), suggesting that the observed Ca^{2+}_i is likely due to activation of specific T2Rs via the denatonium moiety.

Fitting with GPCR activation, denatonium benzoate, and thujone Ca^{2+}_i responses in SCC4 and

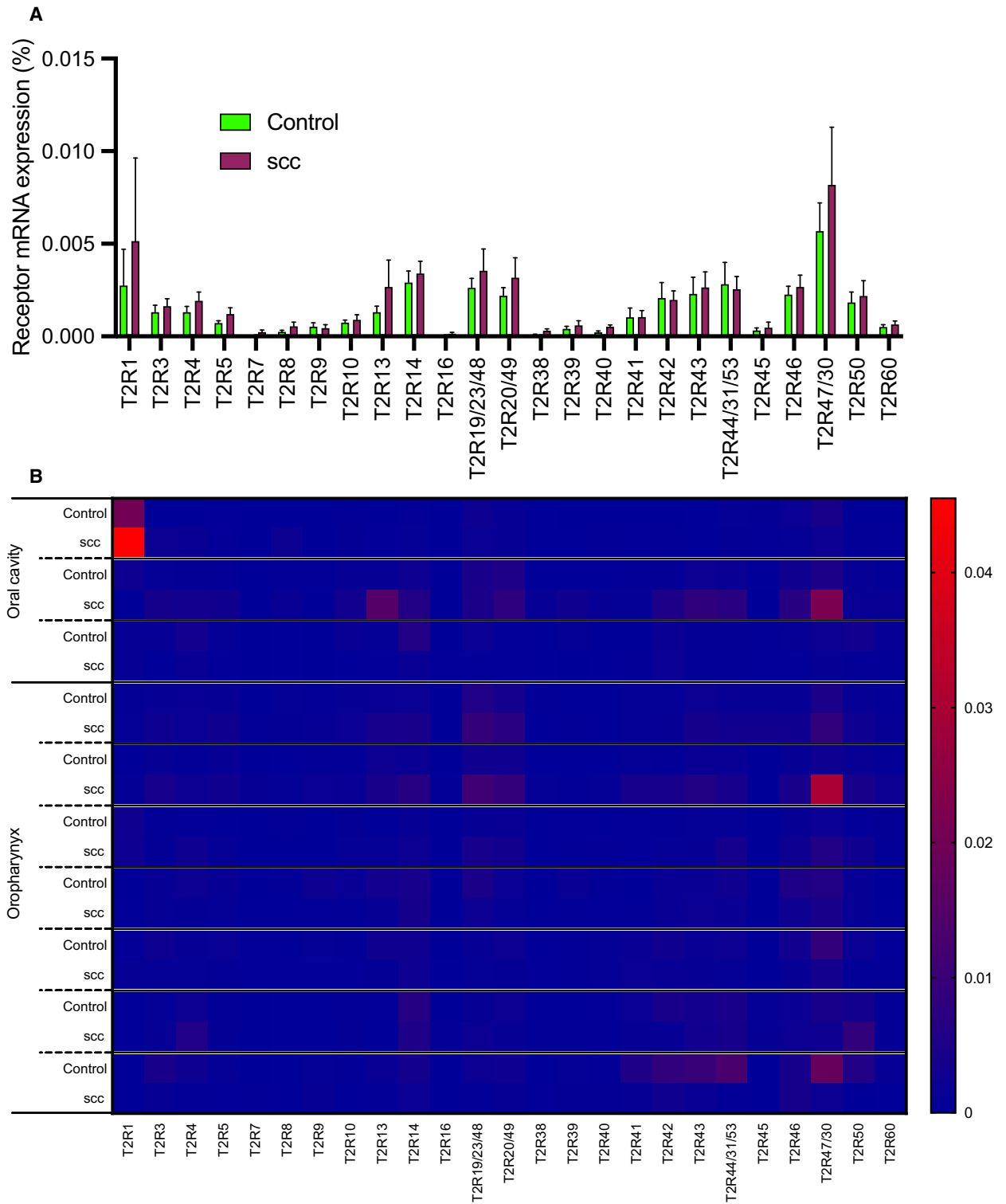


Fig. 1. There is variable mRNA expression of bitter (T2R) taste receptor genes in HNSCC. (A) Quantitative PCR (qPCR) expression analysis of T2R transcripts from biopsy specimens of HNSCC ('SCC') compared with contralateral normal tissue ('control') from the same patient (mean ± SEM; 10 patients). Expression of each *TAS2R* mRNA was normalized to ubiquitin C (UBC) housekeeping gene. No significant differences in individual *TAS2R* gene expression between cancer and control samples by two-way ANOVA with Bonferroni posttest. (B) Heatmap representation of the same T2R transcript data, grouped by individual patients.

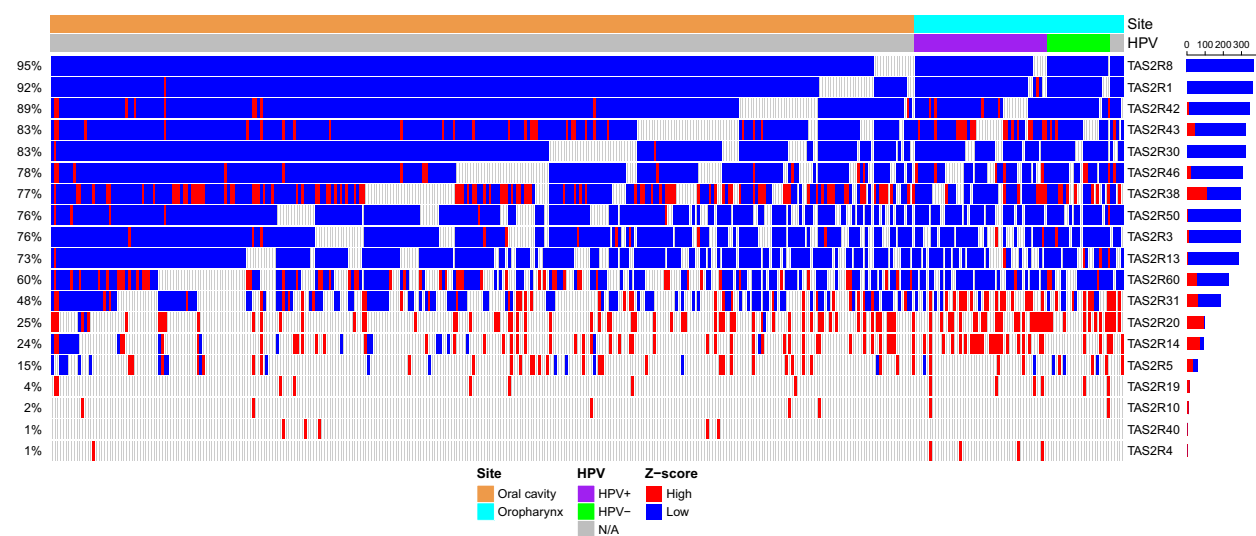


Fig. 2. Bitter taste receptor (*TAS2R*) expression in HNSCC is altered compared with normal tissue. *TAS2R* expression was compared for tumor and adjacent normal tissue in 390 cases of HNSCC of the oral cavity and oropharynx using TCGA [34,35]. *TAS2R* mRNA expression z-scores relative to adjacent normal tissue are shown in the heatmap with z-scores ≥ 2 considered high (red) and z-score ≤ -2 considered low expression (blue). *TAS2R* genes were removed from the plot if they did not have any high or low z-scores across all patients. Data are stratified by oral cavity and oropharynx anatomic sites and by HPV status (HPV+, HPV–, and N/A).

SCC47 cells were inhibited by PLC inhibitor U73122 (Fig. S6A–C). Ca^{2+}_i responses to denatonium benzoate, thujone, and *P. aeruginosa* 3-oxo-C12HSL were also blocked by heterotrimeric G protein inhibitor YM254890 [41] (Fig. S6D–G). Consistent with GPCR-induced PLC activation, Ca^{2+}_i responses to denatonium benzoate and quinine were also blocked with inositol trisphosphate (IP_3) receptor (IP_3R) inhibitor xestospongine C (Fig. S6H–J). Fluo-4 responses to denatonium benzoate were significantly reduced in SCC90 cells stably transfected with shRNA plasmids directed against denatonium-responsive T2R4 (Fig. S7), suggesting T2R4 is important for the denatonium-induced Ca^{2+}_i response.

Fluo-4 responses to denatonium benzoate appeared primarily nuclear (shown for SCC47 in Fig. 4E). This is similar to our studies of airway squamous cells showing T2Rs primarily regulate nuclear calcium ($\text{Ca}^{2+}_{\text{nuc}}$; preprint [39]). To determine whether bitter agonists elevate $\text{Ca}^{2+}_{\text{nuc}}$, SCC47 cells were transfected with nuclear-localized genetically encoded calcium biosensor (R-GECO-nls [34]). Denatonium benzoate (15 mM) and quinine (1 mg·mL⁻¹) triggered $\text{Ca}^{2+}_{\text{nuc}}$ elevation (Fig. 4F,G). Thus, T2Rs in HNSCC cells respond to a wide range of bitter agonists to trigger intracellular and intranuclear Ca^{2+} via G proteins and PLC.

R-GECO-nls $\text{Ca}^{2+}_{\text{nuc}}$ responses to denatonium benzoate were reduced in cells cotransfected with *TAS2R4* shRNA but not *TAS2R14* shRNA (Fig. S8A,C).

T2R14 does not respond to denatonium benzoate [40]. Conversely, $\text{Ca}^{2+}_{\text{nuc}}$ responses to T2R14-specific agonist FFA were reduced with cotransfection of *TAS2R14* shRNAs but not *TAS2R4* shRNAs (Fig. S8B,C). Denatonium-induced $\text{Ca}^{2+}_{\text{nuc}}$ responses were also inhibited by U73122 and YM254980 (Fig. S8D). We noted that $\text{Ca}^{2+}_{\text{nuc}}$ responses were twofold to threefold greater in oral cancer cell lines than in primary oral keratinocytes (Fig. S9).

3.3. Nuclear Ca^{2+} leads to mitochondrial dysfunction and apoptosis

In some cells loaded with Fluo-8, we visualized an initial $\text{Ca}^{2+}_{\text{nuc}}$ response that was followed by a sustained perinuclear response that appeared mitochondrial (Fig. S10). This led us to investigate how bitter agonists affect mitochondrial function in HNSCC cells. $\text{Ca}^{2+}_{\text{nuc}}$ may feed Ca^{2+} to the mitochondria and regulate metabolism or apoptosis [42]. We loaded SCC4 and 47 cells with ratiometric mitochondrial membrane potential ($\Delta\Psi_m$) dye JC-1 and exposed them to denatonium benzoate or quinine over 6 h. Both depolarized $\Delta\Psi_m$, evidenced by a shift in the green-to-red fluorescence ratio (Fig. 5A–D). We also tested $\Delta\Psi_m$ using tetramethylrhodamine ethyl ester (TMRE), which binds only to mitochondria with intact membrane potential. SCC4 cells were treated with denatonium benzoate and quinine for different lengths of time, stained with TMRE and Red Dot 2, and fluorescence

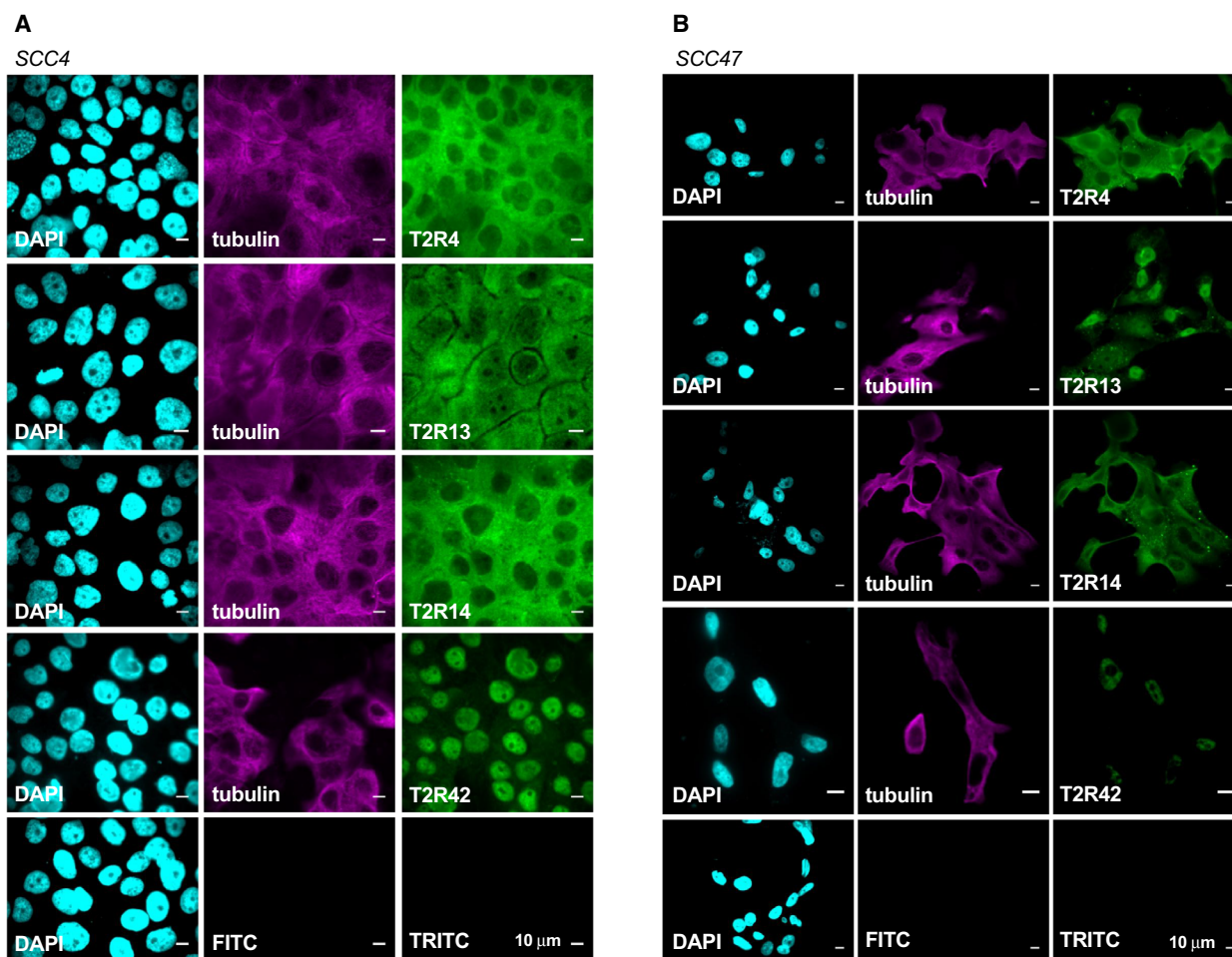


Fig. 3. A subset of T2Rs localize to the nucleus of two HNSCC cell lines. Fixed cultures of HNSCC cell lines (A) SCC4 and (B) SCC47 stained with antibodies targeting endogenous proteins demonstrate nuclear localization of T2R42. T2R13 appears to localize strongly to the nucleus in SCC47 but not in SCC4. T2Rs 4 and 14 are expressed in both cell lines and appear to localize to the plasma membrane. For all images, 1 representative image from 3 experiments was shown. Scale bar represents 10 μm . Each antibody was compared to secondary only control at the same microscope settings.

intensities were compared (Fig. 5E–H). Both bitter agonists led to mitochondrial depolarization and subsequent plasma membrane permeability. Like $\text{Ca}^{2+}_{\text{nuc}}$ responses, denatonium-induced changes in TMRE and JC-1 fluorescence were inhibited by GPCR Ca^{2+} signaling inhibitors U73122 and YM254890 (Fig. S11A–C).

Bitter agonists also decreased cellular metabolism, evidenced by a reduction in NAD(P)H production measured by XTT. In the presence of a cofactor, extracellular XTT is reduced from a nonlight-absorbing to a colored absorbing form by cellular NAD(P)H via cross-plasma-membrane electron transfer. We saw blunted XTT changes 3 h in the presence of 1–10 mM denatonium benzoate in SCC4 and 5–10 mM denatonium benzoate in SCC47 cells.

Primary oral keratinocytes did not exhibit significant changes in XTT at 5–10 mM denatonium benzoate (Fig. 6), fitting with reduced $\text{Ca}^{2+}_{\text{nuc}}$ responses (Fig. S9).

To test whether mitochondrial impairment led to apoptosis, we treated HNSCC cells with a caspase 3/7-sensitive dye (CellEvent caspase 3/7 reagent, Thermo). Exposure to denatonium benzoate caused a significant increase in caspase 3/7 activity over 6 h in SCC4, SCC15, SCC47, and SCC152. Quinine led to a significant increase in SCC4, SCC15, and SCC47, but not SCC152 (Fig. 7). Denatonium-induced caspase 3/7 activity was reduced in the presence of U73122 or YM254890 (Figure S11D,E). Notably, neither denatonium benzoate nor quinine caused significant changes in TMRE fluorescence (measuring mitochondrial

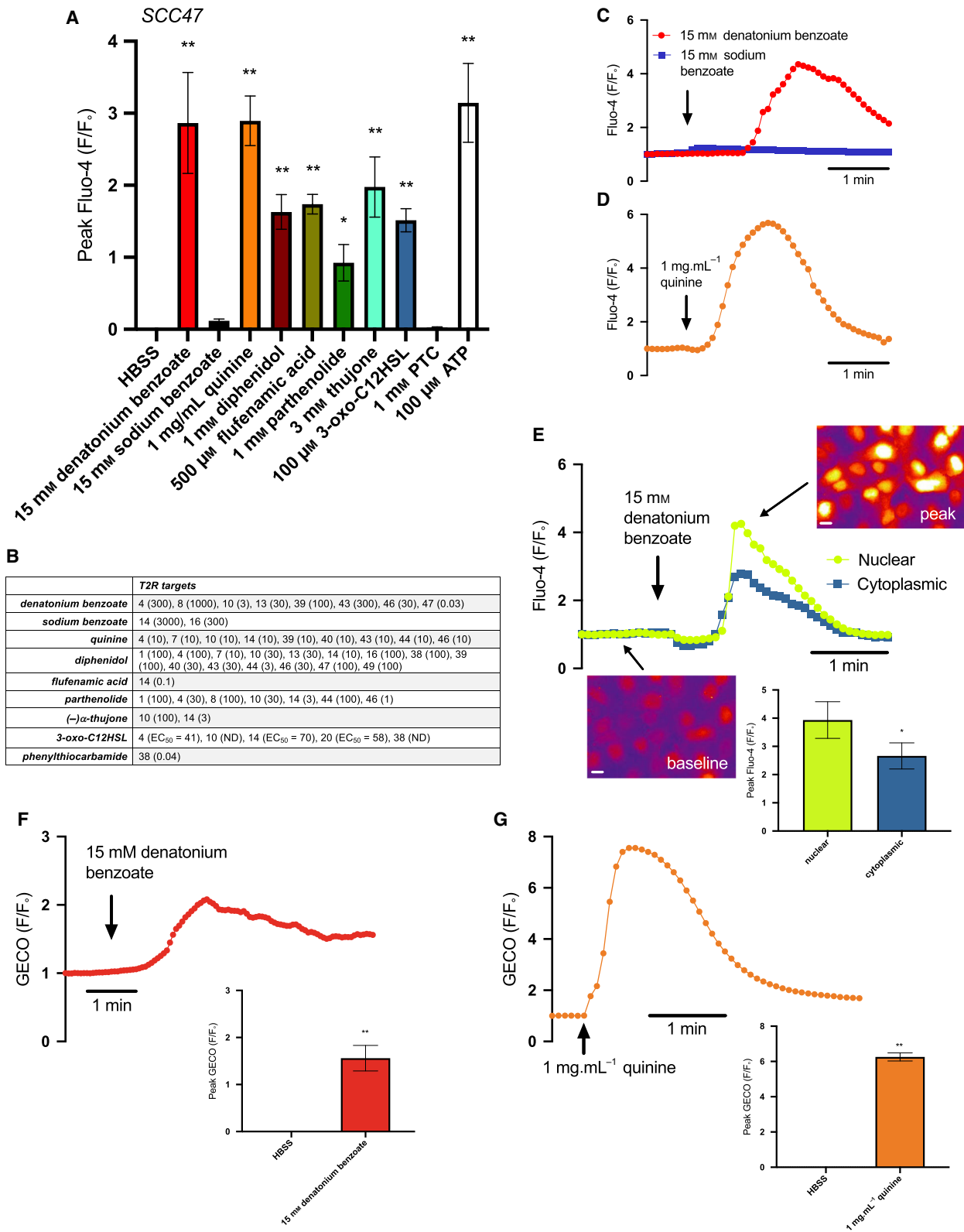


Fig. 4. Bitter (T2R) agonists activate Ca^{2+}_i responses in cultured HNSCC. HNSCC cell line SCC47 loaded with Ca^{2+} binding dye, Fluo-4, was stimulated with T2R agonists, and Ca^{2+} was measured over time. (A) Peak Fluo-4 F/F_0 was quantified after stimulation with Hank's Balanced Salt Solution (HBSS), denatonium benzoate, sodium benzoate, quinine, diphenidol, flufenamic acid, parthenolide, thujone, 3-oxo-C12HSL, phenylthiocarbamide (PTC), and purinergic receptor agonist adenosine triphosphate (ATP) (mean \pm SEM; 3 experiments using separate cultures). Significance by 1-way ANOVA with Bonferroni posttest comparing HBSS to each agonist. (B) Table of T2R targets for agonists used. Effective concentration (EC, in μM) or half-maximal effective concentration (EC_{50} , when indicated) shown in parentheses, taken from [40,50]. Compounds with 'ND' denote EC not determined. (C, D) Representative traces of Fluo-4 F/F_0 over time after stimulation with denatonium benzoate (C) and sodium benzoate (separate traces superimposed) and quinine (D). Traces are from $n = 1$ culture each but are representative of results obtained from 3 independent cultures (mean \pm SEM shown in A). (E) Fluo-4 fluorescence in response to denatonium benzoate-induced Ca^{2+} release appears to localize more strongly to the nucleus than the cytoplasm as represented by the traces and images; peak Fluo-4 F/F_0 for nuclear Ca^{2+} release is significantly greater than cytoplasmic Ca^{2+} release (mean \pm SEM; 3 separate cultures). Significance by unpaired t -test. Scale bar is $10 \mu\text{m}$. (F, G) Nuclear-localized R-GECO-nls was used to measure nuclear Ca^{2+} after stimulation with (F) denatonium benzoate and (G) quinine. Both agonists stimulate nuclear Ca^{2+} as demonstrated by the traces over time and peak GECO F/F_0 compared to HBSS (mean \pm SEM; 3 separate cultures). Significance by unpaired t -test. * $P < 0.05$; ** $P < 0.01$.

potential; Fig. S12A–E) or CellEvent reagent fluorescence (measuring caspase 3/7 activation; Fig. S12F–H) over the same time range that changes were observed with HNSCC cells.

Denatonium benzoate but not sodium benzoate-induced caspase activation was confirmed in HNSCC cells using an optical assay (Flip-GFP; [43]) in SCC4, SCC47, SCC90, and SCC152 cells (Figs S13–S14). Changes in Flip-GFP fluorescence, signaling caspase activation, were blocked by U73122, XeC, or YM254890 (Fig. S14C,D) as well as cotransfection with *TAS2R4* shRNA (Fig. S14E,F).

We further confirmed caspase activation in SCC4 and SCC47 cells using a Förster resonance energy transfer (FRET)-based biosensor created by linking enhanced cyan fluorescent protein (eCFP) and yellow fluorescent protein variant mVenus with a linker containing a DEVD caspase 3 cleavage site [44]. Caspase cleavage of the protein allows the eCFP and mVenus to diffuse farther apart, reducing FRET (Fig. S15A). We saw FRET decreases signaling caspase activation in response to denatonium benzoate, quinine, thujone, 3-oxo-C12HSL, and *Pseudomonas* quinolone signal (PQS) but not sodium benzoate (Fig. S15B–F). In this assay, denatonium benzoate or flufenamic acid-induced caspase activation was reduced by shRNAs against *TAS2R4* or *TAS2R14*, respectively (Fig. S15G–I). Denatonium benzoate-induced executioner caspase activation was also confirmed by western blot for cleaved caspases 3 and 7 (Fig. S16).

Loading SCC4 or SCC47 cells with calcium chelator BAPTA blocked caspase activation, measured by Flip-GFP, in response to denatonium benzoate (Fig. S13G). To determine whether apoptosis was linked to $\text{Ca}^{2+}_{\text{nuc}}$, we utilized a recombinant protein calcium buffer, known as SpiCee [45], fused to either nuclear export or nuclear localization sequences (NES-SpiCee or

NLS-SpiCee, respectively). NLS-SpiCee or NES-SpiCee was cotransfected with the eCFP-DEVD-Venus biosensor (Fig. 7G–H). FRET decreases signaling apoptosis occurred with NES-SpiCee and bitter agonists denatonium benzoate or bacterial 3-oxo-C12HSL (Fig. 7I). However, no apoptosis was observed with NLS-SpiCee. Chelation of $\text{Ca}^{2+}_{\text{nuc}}$ blocked bitter agonist-induced apoptosis (Fig. 7I). Bitter agonist-induced $\text{Ca}^{2+}_{\text{nuc}}$ responses reduce cellular metabolism and proliferation in HNSCC cells.

3.4. Increased *TAS2R* expression may be associated with HNSCC survival

Data above suggest T2Rs activate apoptosis and limit proliferation of HNSCCs *in vitro*, which prompted us to explore possible *in vivo* effects of T2Rs. Specifically, we investigated the impact of increased *TAS2R* expression on survival in HNSCC using TCGA [36,37]. Analysis included 504 cases of HNSCC diagnosed between 1992 and 2013 with mRNA expression data available. *TAS2R* expression z -scores relative to diploid samples are demonstrated in the heatmap in Fig. 8A. Kaplan–Meier survival analysis of cases with high vs low *TAS2R* expression demonstrated improved overall survival for cases with increased *TAS2R* expression ($P = 0.0208$ by log-rank test; Fig. 8B). Median survival was 65.77 months for high *TAS2R* expression versus 39.49 months for low mRNA expression. We also separately evaluated *TAS2R4* expression, as this receptor was expressed in the patient samples and cell lines and is activated by denatonium benzoate and quinine. Kaplan–Meier survival analysis comparing high *TAS2R4* expression and low expression demonstrated improved overall survival for cases with increased *TAS2R4* ($P = 0.0269$ by log-rank test; Fig. 8C). Kaplan–Meier analysis of disease-free survival for

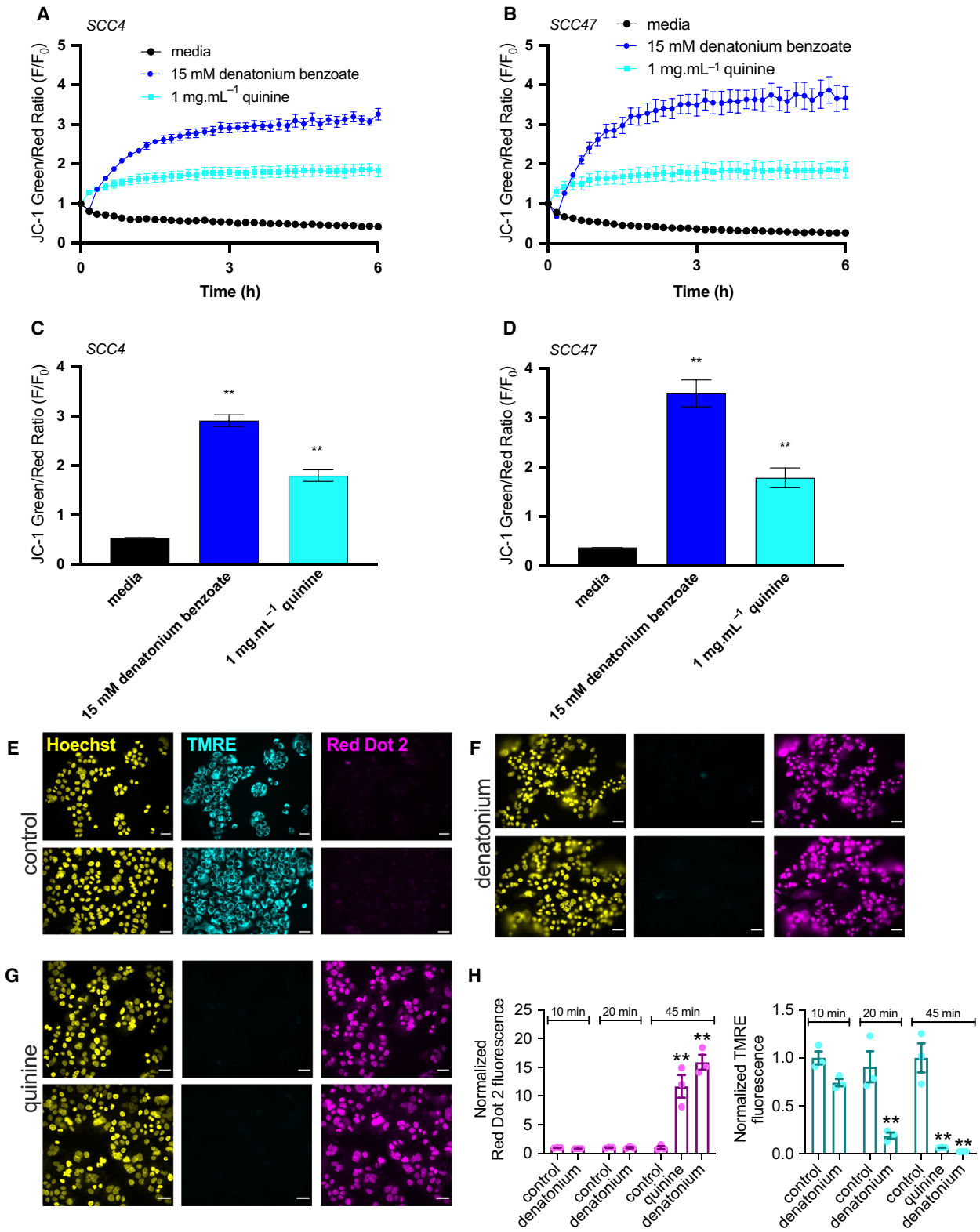


Fig. 5. Bitter (T2R) agonists cause mitochondrial depolarization of HNSCC. JC-1 dye, an indicator of $\Delta\Psi_m$, shows higher green/red signal with depolarized mitochondria. (A–D) SCC cell lines loaded with JC-1 were stimulated with T2R agonists. Representative traces over 6 h for HNSCC cell lines SCC4 (A) and SCC47 (B) after stimulation with media, denatonium benzoate, and quinine demonstrate mitochondrial depolarization with bitter agonists (mean \pm SEM; 3 separate cultures for each cell line). JC-1 green/red ratio was quantified for SCC4 (C) and SCC47 (D) at 3 h showing significantly higher ratios for denatonium benzoate and quinine compared with media (mean \pm SEM; 3 separate cultures for each cell line). Significance by 1-way ANOVA with Bonferroni posttest comparing media to each agonist. (E–H) SCC4 was treated with media (E), denatonium benzoate (F), and quinine (G) for 45 min then stained with Hoechst (nuclei), TMRE (mitochondria with intact membrane potential), and Red Dot 2 (indicates permeable plasma membrane) dyes. Scale bars in E–G are 20 μ m. (H) TMRE and Red Dot 2 fluorescence intensities were separately compared between media, denatonium benzoate, and quinine, demonstrating mitochondrial depolarization and plasma membrane permeability after bitter agonist stimulation (mean \pm SEM; 3 separate cultures). Significance by 1-way ANOVA with Dunnett's posttest comparing media to each agonist. $**P < 0.01$.

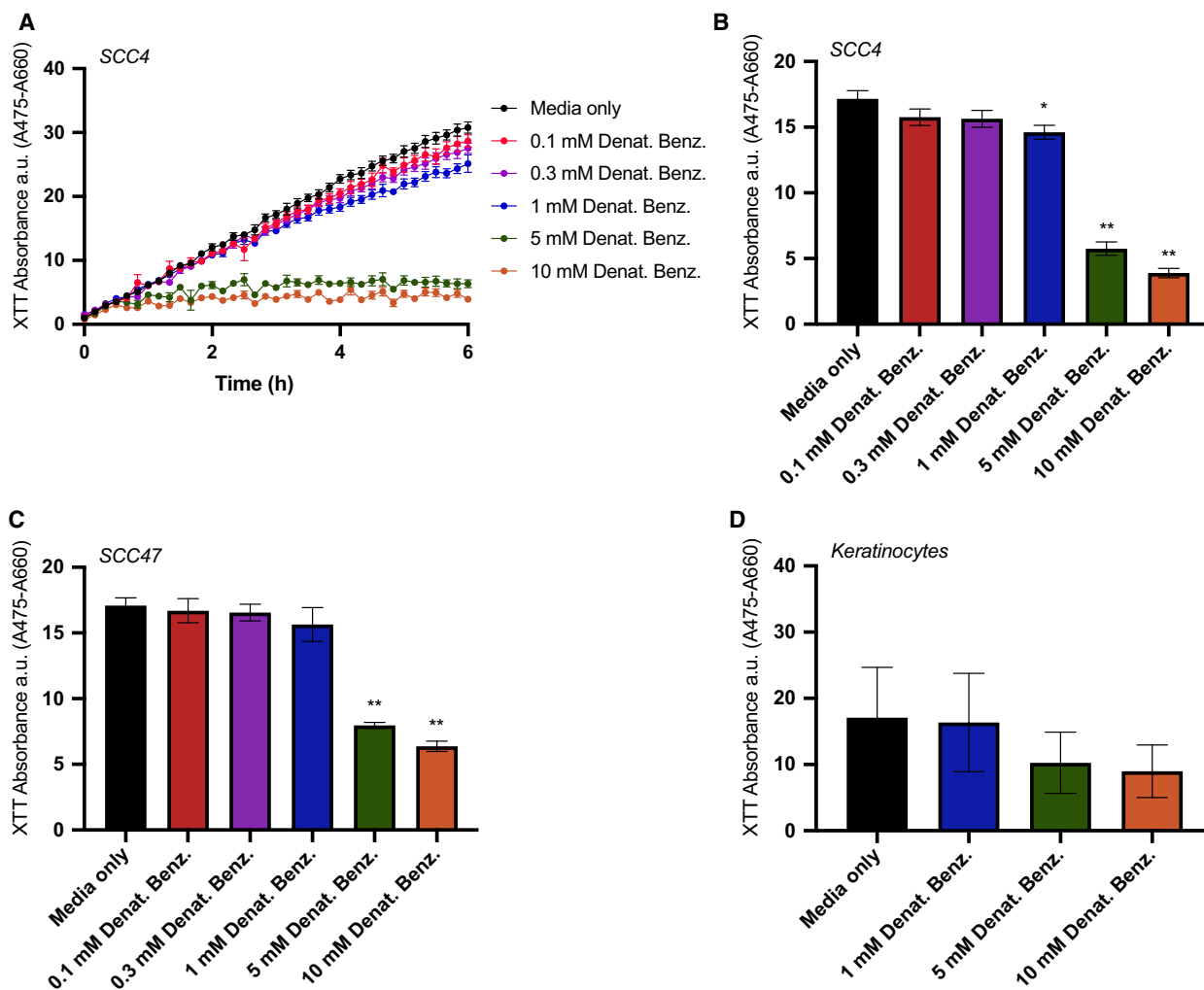


Fig. 6. Bitter (T2R) agonists decrease cellular metabolism in HNSCC. 2,3-bis-(2-methoxy-4-nitro-5-sulfophenyl)-2H-tetrazolium-5-carboxanilide (XTT) was used to measure cellular NAD(P)H production via a cross-plasma-membrane electron transfer. (A) Representative trace over 6 h after stimulation of HNSCC cell line SCC4 with media \pm denatonium benzoate at five different concentrations as indicated (mean \pm SEM; $n = 6$ independent cultures). (B, C) Bar graphs (mean \pm SEM; $n = 6$ independent cultures per cell line) of XTT absorbance quantified at 3 h for (B) SCC4 and (C) SCC47. (D) XTT absorbance quantified at 3 h for primary oral keratinocytes showing smaller (not statistically significant) reduction in NAD(P)H production with denatonium compared with HNSCC cells ($n = 6$ independent cultures from different patients). Significance by 1-way ANOVA with Dunnett's posttest comparing media to each concentration of denatonium benzoate. $*P < 0.05$, $**P < 0.01$.

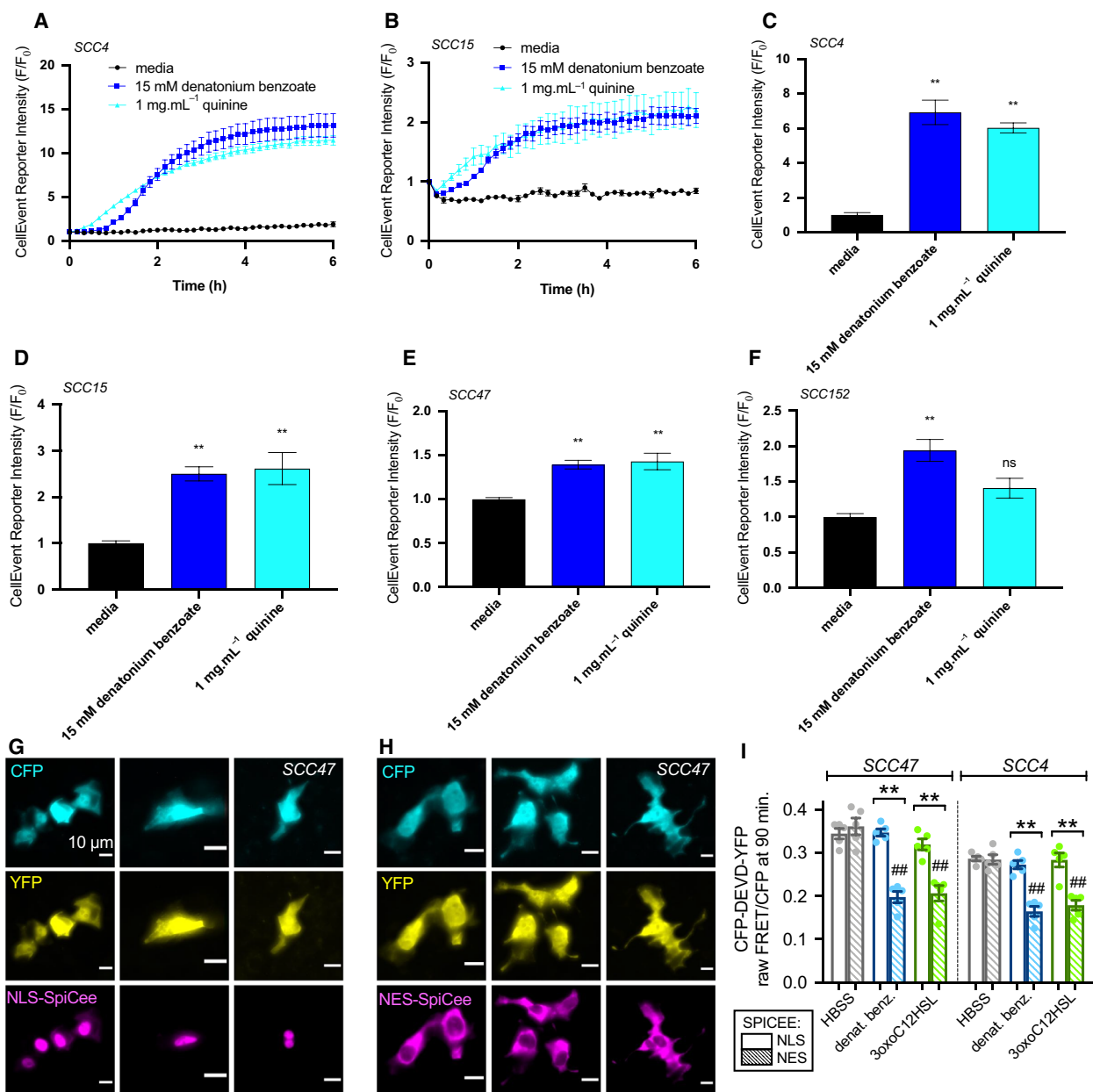


Fig. 7. Bitter (T2R) agonists cause activation of apoptosis in HNSCC. (A, B) Cleavage of caspase 3/7 CellEvent reagent signals apoptosis. Representative traces over 6 h after stimulation of HNSCC cell lines SCC4 (A) and SCC15 (B) with media, denatonium benzoate, and quinine demonstrate increased caspase 3/7 cleavage (mean \pm SEM; 3 separate cultures for SCC4 and 5 separate cultures for SCC15). (C–F) CellEvent reporter intensity at 6 h after stimulation of SCC4 (C), SCC15 (D), SCC47 (E), and SCC152 (F) with bitter agonists, normalized to media (mean \pm SEM; 3 separate cultures for SCC4, SCC47, and SCC152 and 5 separate cultures for SCC15). Significance by 1-way ANOVA with Bonferroni posttest comparing media to each agonist; ** $P < 0.01$, ns = nonsignificant. (G–H) Wide-field 40x fluorescence images of mCherry-labeled NLS-SpiCee (G) or NES-SpiCee (H) cotransfected with caspase FRET biosensor in SCC47 cells. Each column shows cells from a separate individual experiment ($n = 3$ for each condition shown), but results representative of results from 5 independent experiments (averaged in I). Scale bars in G and H are 10 μ m. (I) FRET ratios were measured in cells after 90-min incubation with HBSS (gray bars), 10 mM denatonium benzoate (blue bars), or 100 μ M 3-oxo-C12HSL (green bars). Open bars are NLS-SpiCee, and crossed bars are NES-SpiCee. A downward deflection indicates loss of FRET signal signifying caspase cleavage. Each data point is an independent experiment. Graph shows mean \pm SEM of 5 independent experiments with each cell line. Each independent experiment imaged 5–9 cells from a single field of view. Significance by one-way ANOVA with Bonferroni posttest; ** $P < 0.01$ between bracketed bars; ### $P < 0.01$ compared with HBSS.

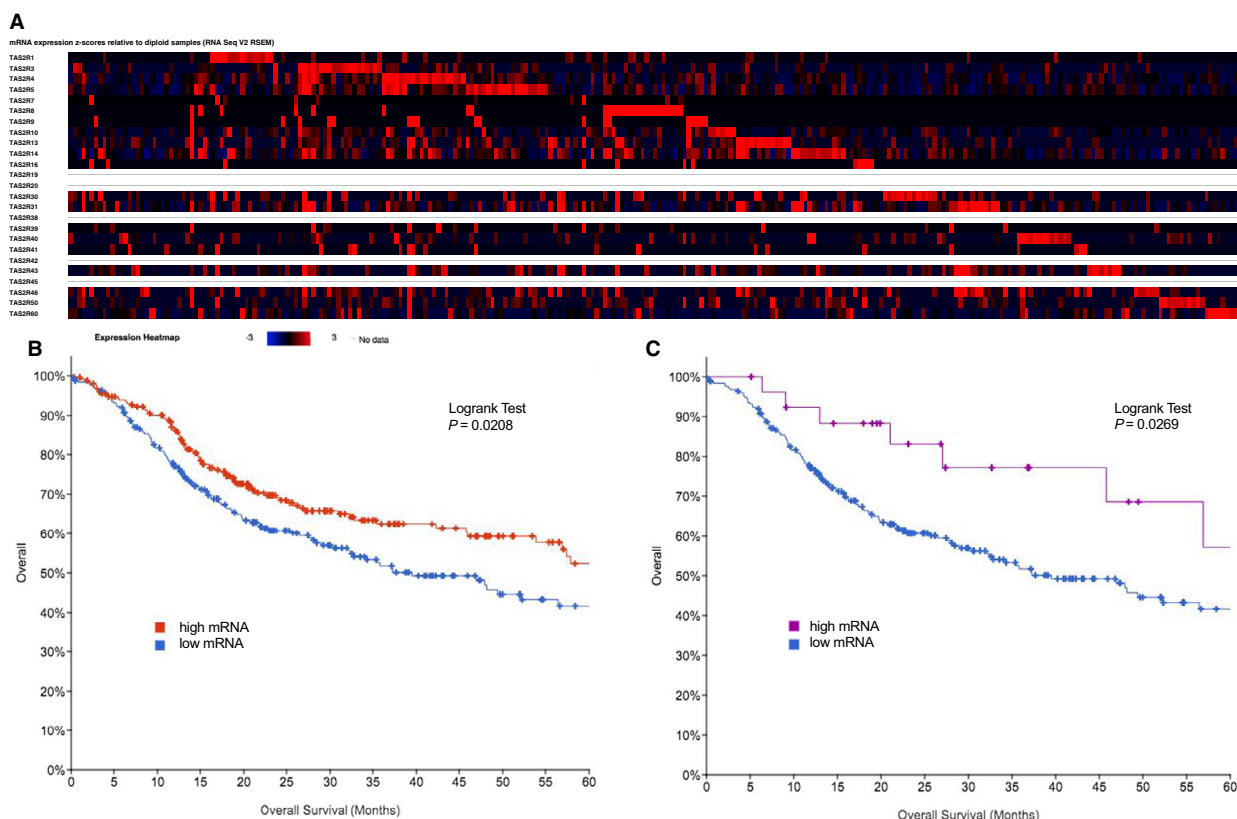


Fig. 8. Bitter taste receptor (*TAS2R*) expression alterations in HNSCC are associated with survival. *TAS2R* expression alterations were analyzed for 504 cases of HNSCC using TCGA [36,37]. (A) Heatmap of *TAS2R* mRNA expression z-scores relative to diploid samples. Increased *TAS2R* expression (red) is more common than decreased expression (blue). (B) 5-year survival analysis of HNSCC cases demonstrates that increased *TAS2R* expression is associated with improved overall survival ($P = 0.0208$ by log-rank test). (C) Increased *TAS2R4* expression, which is activated by the bitter agonists denatonium benzoate, quinine, diphenidol, parthenolide, and 3-oxo-C12HSL, is also associated with improved overall survival ($P = 0.0269$ by log-rank test).

TAS2R and *TAS2R4* expression alterations did not show a statistically significant difference ($P = 0.896$ and 0.837 by log-rank test, respectively; Fig. S17).

Evaluation of genetic changes in addition to expression changes showed that 283 out of 504 cases (56.15%) had some *TAS2R* alteration (Fig. S18A). Multiple alterations were present in 11.51% of cases (Fig. S18B). Kaplan–Meier survival analysis of cases with and without *TAS2R* genetic alterations showed improved survival for patients with genetic alterations which was not statistically significant ($p = 0.0891$ by log-rank test; Fig. S18C). Similarly, there was improved disease-free survival for patients with genetic alterations which was not statistically significant ($P = 0.111$ by log-rank test; Fig. S18D).

TCGA analyses suggest *TAS2R* genetic and expression alterations are prevalent in HNSCC. Increased *TAS2R* expression may be beneficial by limiting cancer cell proliferation via mechanisms outlined above.

4. Discussion

While T2Rs have been studied in cancer [14–23], this is the first description of T2R expression and signaling in HNSCC. Bitter agonists activate T2R-mediated $\text{Ca}^{2+}_{\text{nuc}}$, which triggers mitochondrial depolarization, caspase activation, and apoptosis. The novel demonstration of a requirement for $\text{Ca}^{2+}_{\text{nuc}}$ in bitter agonist-induced apoptosis may be important to other cancers. Using TCGA, we report that increased *TAS2R* expression is correlated with HNSCC survival, suggesting potential clinical utility of T2R agonists and supporting future prospective studies in larger patient populations to test if/how T2Rs are diagnostic biomarkers in HNSCC.

The *TAS2Rs* with highest expression in HNSCC (*TAS2R4*, *TAS2R14*, *TAS2R19*, *TAS2R20*, *TAS2R30*, *TAS2R43*, and *TAS2R45*) overlap with *TAS2Rs* expressed at increased levels in breast cancer [20,21].

However, the concept of T2R expression on the nuclear membrane is highly novel. We (preprint [39]) and others [46] have found nuclear localization of T2Rs in deciliated or inflamed airway tissues. We also saw this in lung cancer cells (preprint [39]). Squamous dedifferentiation likely alters localization of airway T2Rs from cilia to the nucleus, where T2Rs activate $\text{Ca}^{2+}_{\text{nuc}}$ and apoptosis rather than ciliary beating activated in differentiated healthy tissues [11,35]. HNSCC cells also have at least some nuclear T2Rs. Prior studies have validated importance of nuclear envelope GPCRs in neurons and other cells [47–49], but the link between intracellular T2Rs, $\text{Ca}^{2+}_{\text{nuc}}$, and apoptosis in cancer cells is novel. Notably, Ca^{2+} can be regulated by GPCRs directly within the nucleus as well as on surrounding ER and/or nuclear envelope membranes ([47–49]). While more detailed subcellular localization studies are needed, more work is also required to determine potential functional differences of T2R isoforms beyond localization. A detailed study of the localization of all 25 T2R isoforms is needed in future studies.

Interestingly, orphan T2R42 [40,50] localized to the nucleus in two HNSCC tongue cell lines. Understanding T2R42 function will be difficult with no known agonists, but *TAS2R42* expression in tumor compared with normal tissue was altered in $\sim 89\%$ of oral and oropharyngeal cancers in our TCGA analysis. Understanding whether orphan T2Rs such as T2R42 have endogenous or bacteria-derived bitter agonists is also critical to interpreting their role in HNSCC cells. Constitutive activity has been described for some mutated T2Rs [51]. One possibility, unsupported but intriguing is that orphan T2Rs may have constitutive activity that plays a role in baseline cell proliferation and/or metabolism.

Further work is needed to determine specific subcellular localizations of each T2R isoform. Combined with knockout studies, this may reveal other novel functions beyond activation of apoptosis in HNSCC cells. Several T2Rs that are activated by denatonium benzoate or quinine (including T2Rs 4, 8, 10, 14, 30/47, and 46) did not localize to the nucleus, but nonetheless appeared intracellular. T2R13, activated by denatonium benzoate [40,50], was nuclear in SCC47 but not in SCC4. Thus, differences in T2R localization between cancers of the same anatomic site may exist. It is interesting that the denatonium-induced Ca^{2+} response is strongly dependent on T2R4 despite expression of other denatonium-responsive T2Rs (e.g., T2R30 and T2R13) in HNSCC cells. It may be that these T2Rs are not linked to Ca^{2+} but are instead linked to other pathways in these cells. Or, it

may be that mRNA expression levels do not correlate with protein expression levels. Further work is needed to understand whether all T2R isoforms signal similarly in cancer cells, as much of our knowledge of T2R signaling is based on taste bud cells or heterologous expression systems using chimeric G proteins that force T2Rs to couple to calcium. While useful for screening bitter compounds, these assays cannot reveal differences in endogenous T2R signaling.

Multi-T2R targeting compounds such as denatonium benzoate or quinine might be useful to activate apoptosis in HNSCCs from a broad range of patients. Many known T2R agonists (e.g., quinine) are cell permeant [52,53]. Intracellular T2Rs could be targeted using high-dose topical treatments in accessible anatomic locations like the oral cavity/oropharynx. Many pharmaceuticals with known safety profiles are bitter [54] and could potentially kill or slow the growth of HNSCC, particularly if specific T2R agonists can be used in combination with genetic profiling to determine expression of specific T2Rs in tumor vs normal tissue.

$\text{Ca}^{2+}_{\text{nuc}}$ and cytosolic Ca^{2+} are distinct, but both are activated by ryanodine receptors and IP_3Rs [55,56]. $\text{Ca}^{2+}_{\text{nuc}}$ responses to bitter agonists in HNSCC originate partly from the ER, requiring PLC and IP_3Rs . Nuclear Ca^{2+} regulates transcription factors but was also linked to apoptosis [57–59]. Bitter agonists activate apoptosis and/or mitochondrial depolarization in other cell types [60–63], including metastatic breast cancer [64], prostate cancer [65], and acute myeloid leukemia cells [61]. In pancreatic cancer, T2R38 can be activated by 3-oxo-C12HSL [19], suggesting a possible link with the microbiome. In contrast, denatonium benzoate had protumor actions in murine submandibular gland cancer cells [18]. We show here that bitter agonists, including bacterial 3-oxo-C12HSL and PQS, are antiproliferative and proapoptotic in HNSCC, with a novel mechanistic link between $\text{Ca}^{2+}_{\text{nuc}}$ and apoptosis.

TCGA analysis suggests *TAS2R* expression alterations impact HNSCC or serve as markers of underlying genetic changes that contribute to tumor biology and treatment efficacy. *TAS2R* expression alterations are associated with better survival. We hypothesize that, as T2Rs regulate apoptosis, tumors that overexpress T2Rs may have an improved prognosis due to a more robust internal regulation preventing unchecked proliferation or responding to bitter agonists in the microenvironment, either from the tumor microbiome or intracellular metabolites.

We did not detect an association of *TAS2R* expression and disease-free survival, suggesting that T2Rs

may be associated with longer survival but not necessarily disease control. We also did not appreciate anatomic or HPV-related differences in *TAS2R* expression, suggesting that expression may vary independently of anatomic site or that an even larger sample size may be needed to detect more subtle differences. Further work is necessary to appreciate the full impact of T2Rs in HNSCC and potential roles in risk stratification and treatment. Furthermore, common genetic polymorphisms in *TAS2Rs* that affect bitter taste perception and dietary preferences [66,67] may contribute to differences in tumor behavior. Long-term prospective clinical studies that include multivariate analyses and evaluation of patient and disease factors (e.g., smoking, sex, and tumor stage) are still needed to further clarify the predictive value of T2Rs in HSNCC.

Identification of prognostic markers to guide treatment selection is an active area of HNSCC research to ultimately improve survival while mitigating treatment-related side effects. Several clinical trials have sought to limit treatment-related morbidity by de-intensifying therapy in HPV-associated oropharyngeal tumors, which are known to have improved prognosis compared with HPV-negative tumors [68,69]. If increased *TAS2R* expression portends favorable prognoses, it would be reasonable to perform *TAS2R* expression analysis of HNSCC tumors as part of the treatment selection algorithm, similar to standard practice HPV testing for oropharyngeal SCCs.

Importantly, bacterial ligands such as PQS or 3-oxo-C12HSL are hydrophobic and cell permeant [70,71]. These molecules can reach $\geq 100 \mu\text{M}$ in localized bacterial environments [72]. Thus, intracellular T2Rs could be activated by these bacterial metabolites. We propose that cancer cell T2Rs may link the host microbiome with HNSCC progression. HNSCCs are known to be associated with unique microbiomes [73–77], impacting the immune system and contributing to oncogenesis and oncologic outcomes [73,78,79]. T2R-mediated recognition of bacterial ligands and resulting interkingdom signaling may play a role in HNSCC and other cancer pathophysiology.

5. Conclusions

Our data demonstrate that HNSCC cells express functional T2Rs on the cell membrane and nucleus which respond to bitter compounds, including bacterial metabolites. Activation of these T2Rs leads to nuclear Ca^{2+} responses, mitochondrial depolarization, caspase activation, and apoptosis. TCGA data suggest that increased expression of *TAS2Rs* in HNSCCs is

associated with improved overall survival, possibly related to the role of T2Rs in limiting cancer cell proliferation. Future work will be necessary to determine whether this class of receptors can serve as biomarkers for oncologic outcomes or therapeutic targets for selective activation of apoptosis in cancer cells.

Acknowledgements

We thank Maureen Victoria (University of Pennsylvania) for technical assistance and Noam Cohen (University of Pennsylvania) for advice and discussion. We thank Dr. Hans Joenje (VU Medical Center, the Netherlands) for providing VU147T cells. This study was supported by National Institute of Health Grant R01DC016309 to RJL and pilot funding from the Department of Otorhinolaryngology (University of Pennsylvania) and the American Head and Neck Society to RMC. The funders had no role in study design, data collection, analysis, writing, or decision to submit.

Conflict of interest

The authors declare no conflict of interest.

Data accessibility

All data will be provided under Data Transfer Agreement upon reasonable request to RJL (rjl@penn-medicine.upenn.edu).

Author contributions

RMC, KTN, EAW, and RJL conceptualized and visualized the study; RMC, DBM, ZAM, IG, TBK, and RJL investigated and involved in formal analysis; RMC wrote—original draft; RMC, TBK, EAW, and RJL wrote—review and editing; KR, JGN, and DB curated the data and contributed to resources; RMC and RJL involved in funding acquisition; RJL supervised the study.

References

- 1 Johnson DE, Burtness B, Leemans CR, Lui VWY, Bauman JE & Grandis JR (2020) Head and neck squamous cell carcinoma. *Nat Rev Dis Primers* **6**, 92.
- 2 Jou A & Hess J (2017) Epidemiology and molecular biology of head and neck cancer. *Oncol Res Treat* **40**, 328–332.
- 3 Kamangar F, Dores GM & Anderson WF (2006) Patterns of cancer incidence, mortality, and prevalence

- across five continents: defining priorities to reduce cancer disparities in different geographic regions of the world. *J Clin Oncol* **24**, 2137–2150.
- 4 Cramer JD, Burtneß B & Ferris RL (2019) Immunotherapy for head and neck cancer: Recent advances and future directions. *Oral Oncol* **99**, 104460.
 - 5 Network NCC (2019) Head and Neck Cancers (Version 2.2019).
 - 6 Lazarus CL (2009) Effects of chemoradiotherapy on voice and swallowing. *Curr Opin Otolaryngol Head Neck Surg* **17**, 172–178.
 - 7 Ang KK, Harris J, Wheeler R, Weber R, Rosenthal DI, Nguyen-Tan PF, Westra WH, Chung CH, Jordan RC, Lu C *et al.* (2010) Human papillomavirus and survival of patients with oropharyngeal cancer. *N Engl J Med* **363**, 24–35.
 - 8 Weinberger PM, Yu Z, Haffty BG, Kowalski D, Harigopal M, Brandsma J, Sasaki C, Joe J, Camp RL, Rimm DL *et al.* (2006) Molecular classification identifies a subset of human papillomavirus-associated oropharyngeal cancers with favorable prognosis. *J Clin Oncol* **24**, 736–747.
 - 9 Janssen S, Laermans J, Verhulst PJ, Thijs T, Tack J & Depoortere I (2011) Bitter taste receptors and alpha-gustducin regulate the secretion of ghrelin with functional effects on food intake and gastric emptying. *Proc Natl Acad Sci USA* **108**, 2094–2099.
 - 10 Carey RM & Lee RJ (2019) Taste receptors in upper airway innate immunity. *Nutrients* **11**, 2017.
 - 11 Hariri BM, McMahon DB, Chen B, Freund JR, Mansfield CJ, Doghramji LJ, Adappa ND, Palmer JN, Kennedy DW, Reed DR *et al.* (2017) Flavones modulate respiratory epithelial innate immunity: anti-inflammatory effects and activation of the T2R14 receptor. *J Biol Chem* **292**, 8484–8497.
 - 12 Bachmanov AA, Bosak NP, Lin C, Matsumoto I, Ohmoto M, Reed DR & Nelson TM (2014) Genetics of taste receptors. *Curr Pharm Des* **20**, 2669–2683.
 - 13 Gopallawa I, Freund JR & Lee RJ (2020) Bitter taste receptors stimulate phagocytosis in human macrophages through calcium, nitric oxide, and cyclic-GMP signaling. *Cell Mol Life Sci* **78**, 271–286.
 - 14 Barontini J, Antinucci M, Tofanelli S, Cammalleri M, Dal Monte M, Gemignani F, Vodicka P, Marangoni R, Vodickova L, Kupcinskas J *et al.* (2017) Association between polymorphisms of TAS2R16 and susceptibility to colorectal cancer. *BMC Gastroenterol* **17**, 104.
 - 15 Carrai M, Steinke V, Vodicka P, Pardini B, Rahner N, Holinski-Feder E, Morak M, Schackert HK, Görgens H, Stemmler S *et al.* (2011) Association between TAS2R38 gene polymorphisms and colorectal cancer risk: a case-control study in two independent populations of Caucasian origin. *PLoS One* **6**, e20464.
 - 16 Choi JH, Lee J, Choi IJ, Kim YW, Ryu KW & Kim J (2016) Genetic variation in the TAS2R38 bitter taste receptor and gastric cancer risk in Koreans. *Sci Rep* **6**, 26904.
 - 17 Choi JH, Lee J, Yang S, Lee EK, Hwangbo Y & Kim J (2018) Genetic variations in TAS2R3 and TAS2R4 bitterness receptors modify papillary carcinoma risk and thyroid function in Korean females. *Sci Rep* **8**, 15004.
 - 18 Dmytrenko G, Castro ME & Sales ME (2017) Denatonium and naringenin promote SCA-9 tumor growth and angiogenesis: participation of arginase. *Nutr Cancer* **69**, 780–790.
 - 19 Gaida MM, Mayer C, Dapunt U, Stegmaier S, Schirmacher P, Wabnitz GH & Hänsch GM (2016) Expression of the bitter receptor T2R38 in pancreatic cancer: localization in lipid droplets and activation by a bacteria-derived quorum-sensing molecule. *Oncotarget* **7**, 12623–12632.
 - 20 Jaggupilli A, Singh N, Upadhyaya J, Sikarwar AS, Arakawa M, Dakshinamurti S, Bhullar RP, Duan K & Chelikani P (2017) Analysis of the expression of human bitter taste receptors in extraoral tissues. *Mol Cell Biochem* **426**, 137–147.
 - 21 Singh N, Chakraborty R, Bhullar RP & Chelikani P (2014) Differential expression of bitter taste receptors in non-cancerous breast epithelial and breast cancer cells. *Biochem Biophys Res Comm* **446**, 499–503.
 - 22 Stern L, Giese N, Hackert T, Strobel O, Schirmacher P, Felix K & Gaida MM (2018) Overcoming chemoresistance in pancreatic cancer cells: role of the bitter taste receptor T2R10. *Journal of Cancer* **9**, 711–725.
 - 23 Yamaki M, Saito H, Isono K, Goto T, Shirakawa H, Shoji N, Satoh-Kuriwada S, Sasano T, Okada R, Kudoh K *et al.* (2017) Genotyping analysis of bitter-taste receptor genes TAS2R38 and TAS2R46 in Japanese patients with gastrointestinal cancers. *J Nutr Sci Vitaminol* **63**, 148–154.
 - 24 Lambert JD, VanDusen SR, Cockroft JE, Smith EC, Greenwood DC & Cade JE (2019) Bitter taste sensitivity, food intake, and risk of malignant cancer in the UK Women's Cohort Study. *Eur J Nutr* **58**, 2111–2121.
 - 25 Sriram K, Moyung K, Corriden R, Carter H & Insel PA (2019) GPCRs show widespread differential mRNA expression and frequent mutation and copy number variation in solid tumors. *PLoS Biol* **17**, e3000434.
 - 26 Carey RM, Freund JR, Hariri BM, Adappa ND, Palmer JN & Lee RJ (2020) Polarization of protease-activated receptor 2 (PAR-2) signaling is altered during airway epithelial remodeling and deciliation. *J Biol Chem* **295**, 6721–6740.
 - 27 McMahon DB, Carey RM, Kohanski MA, Adappa ND, Palmer JN & Lee RJ (2021) PAR-2-activated secretion by airway gland serous cells: role for CFTR

- and inhibition by *Pseudomonas aeruginosa*. *Am J Physiol Lung Cell Mol Physiol* **320**, L845–L879.
- 28 McMahon DB, Carey RM, Kohanski MA, Tong CCL, Papagiannopoulos P, Adappa ND, Palmer JN & Lee RJ (2020) Neuropeptide regulation of secretion and inflammation in human airway gland serous cells. *Eur Respir J* **55**, 1901386.
 - 29 McMahon DB, Workman AD, Kohanski MA, Carey RM, Freund JR, Hariri BM, Chen B, Doghramji LJ, Adappa ND, Palmer JN *et al.* (2018) Protease-activated receptor 2 activates airway apical membrane chloride permeability and increases ciliary beating. *FASEB J* **32**, 155–167.
 - 30 Basu D, Nguyen TT, Montone KT, Zhang G, Wang LP, Diehl JA, Rustgi AK, Lee JT, Weinstein GS & Herlyn M (2010) Evidence for mesenchymal-like subpopulations within squamous cell carcinomas possessing chemoresistance and phenotypic plasticity. *Oncogene* **29**, 4170–4182.
 - 31 Begum S, Gillison ML, Ansari-Lari MA, Shah K & Westra WH (2003) Detection of human papillomavirus in cervical lymph nodes: a highly effective strategy for localizing site of tumor origin. *Clin Cancer Res* **9**, 6469–6475.
 - 32 Christensen JN, Schmidt H, Steiniche T & Madsen M (2020) Identification of robust reference genes for studies of gene expression in FFPE melanoma samples and melanoma cell lines. *Melanoma Res* **30**, 26–38.
 - 33 Chua SL, See Too WC, Khoo BY & Few LL (2011) UBC and YWHAZ as suitable reference genes for accurate normalisation of gene expression using MCF7, HCT116 and HepG2 cell lines. *Cytotechnology* **63**, 645–654.
 - 34 Zhao Y, Araki S, Wu J, Teramoto T, Chang YF, Nakano M, Abdelfattah AS, Fujiwara M, Ishihara T, Nagai T *et al.* (2011) An expanded palette of genetically encoded Ca(2)(+) indicators. *Science* **333**, 1888–1891.
 - 35 Freund JR, Mansfield CJ, Doghramji LJ, Adappa ND, Palmer JN, Kennedy DW, Reed DR, Jiang P & Lee RJ (2018) Activation of airway epithelial bitter taste receptors by *Pseudomonas aeruginosa* quinolones modulates calcium, cyclic-AMP, and nitric oxide signaling. *J Biol Chem* **293**, 9824–9840.
 - 36 Cerami E, Gao J, Dogrusoz U, Gross BE, Sumer SO, Aksoy BA, Jacobsen A, Byrne CJ, Heuer ML, Larsson E *et al.* (2012) The cBio cancer genomics portal: an open platform for exploring multidimensional cancer genomics data. *Cancer Discov* **2**, 401–404.
 - 37 Gao J, Aksoy BA, Dogrusoz U, Dresdner G, Gross B, Sumer SO, Sun Y, Jacobsen A, Sinha R, Larsson E *et al.* (2013) Integrative analysis of complex cancer genomics and clinical profiles using the cBioPortal. *Sci Signal* **6**, p11.
 - 38 Chakravarthy A, Henderson S, Thirdborough SM, Ottensmeier CH, Su X, Lechner M, Feber A, Thomas GJ & Fenton TR (2016) Human papillomavirus drives tumor development throughout the head and neck: improved prognosis is associated with an immune response largely restricted to the oropharynx. *J Clin Oncol* **34**, 4132–4141.
 - 39 McMahon DB, Kuek LE, Johnson ME, Johnson PO, Horn RLJ, Carey RM, Adappa ND, Palmer JN & Lee RJ. (2021) The bitter end: T2R bitter receptor agonists elevate nuclear calcium and induce apoptosis in non-ciliated airway epithelial cells. *bioRxiv* 1–36.
 - 40 Meyerhof W, Batram C, Kuhn C, Brockhoff A, Chudoba E, Bufe B, Appendino G & Behrens M (2010) The molecular receptive ranges of human TAS2R bitter taste receptors. *Chem Senses* **35**, 157–170.
 - 41 Tietze D, Kaufmann D, Tietze AA, Voll A, Reher R, König G & Hausch F (2019) Structural and dynamical basis of G protein inhibition by YM-254890 and FR900359: an inhibitor in action. *J Chem Inf Model* **59**, 4361–4373.
 - 42 Nicotera P, Zhivotovsky B & Orrenius S (1994) Nuclear calcium transport and the role of calcium in apoptosis. *Cell Calcium* **16**, 279–288.
 - 43 Zhang Q, Schepis A, Huang H, Yang J, Ma W, Torra J, Zhang SQ, Yang L, Wu H, Nonell S *et al.* (2019) Designing a green fluorogenic protease reporter by flipping a beta strand of GFP for imaging apoptosis in animals. *J Am Chem Soc* **141**, 4526–4530.
 - 44 Albeck JG, Burke JM, Spencer SL, Lauffenburger DA & Sorger PK (2008) Modeling a snap-action, variable-delay switch controlling extrinsic cell death. *PLoS Biol* **6**, 2831–2852.
 - 45 Ros O, Baudet S, Zagar Y, Loulier K, Roche F, Couvet S, Aghaie A, Atkins M, Louail A, Petit C *et al.* (2020) SpiCee: a genetic tool for subcellular and cell-specific calcium manipulation. *Cell Rep* **32**, 107934.
 - 46 Zborowska-Piskadlo K, Stachowiak M, Rusetska N, Sarnowska E, Siedlecki J & Dzaman K (2020) The expression of bitter taste receptor TAS2R38 in patients with chronic rhinosinusitis. *Arch Immunol Ther Exp (Warsz)* **68**, 26.
 - 47 Crilly SE & Puthenveedu MA (2020) Compartmentalized GPCR signaling from intracellular membranes. *J Membr Biol* **254**, 259–271.
 - 48 Jong YI, Harmon SK & O'Malley KL (2018) GPCR signalling from within the cell. *Br J Pharmacol* **175**, 4026–4035.
 - 49 Ribeiro-Oliveira R, Vojtek M, Goncalves-Monteiro S, Vieira-Rocha MS, Sousa JB, Goncalves J & Diniz C (2019) Nuclear G-protein-coupled receptors as putative novel pharmacological targets. *Drug Discov Today* **24**, 2192–2201.
 - 50 Wiener A, Shudler M, Levit A & Niv MY (2012) BitterDB: a database of bitter compounds. *Nucleic Acids Res* **40**, D413–419.

- 51 Pydi SP, Bhullar RP & Chelikani P (2014) Constitutive activity of bitter taste receptors (T2Rs). *Adv Pharmacol* **70**, 303–326.
- 52 Peri I, Mamrud-Brains H, Rodin S, Krizhanovsky V, Shai Y, Nir S & Naim M (2000) Rapid entry of bitter and sweet tastants into liposomes and taste cells: implications for signal transduction. *Am J Physiol Cell Physiol* **278**, C17–25.
- 53 Zubare-Samuelov M, Shaul ME, Peri I, Aliluiko A, Tirosch O & Naim M (2005) Inhibition of signal termination-related kinases by membrane-permeant bitter and sweet tastants: potential role in taste signal termination. *Am J Physiol Cell Physiol* **289**, C483–492.
- 54 Levit A, Nowak S, Peters M, Wiener A, Meyerhof W, Behrens M & Niv MY (2014) The bitter pill: clinical drugs that activate the human bitter taste receptor TAS2R14. *FASEB J* **28**, 1181–1197.
- 55 Gomes DA, Leite MF, Bennett AM & Nathanson MH (2006) Calcium signaling in the nucleus. *Can J Physiol Pharmacol* **84**, 325–332.
- 56 Rodrigues MA, Gomes DA, Nathanson MH & Leite MF (2009) Nuclear calcium signaling: a cell within a cell. *Braz J Med Biol Res* **42**, 17–20.
- 57 Gerasimenko OV, Gerasimenko JV, Tepikin AV & Petersen OH (1996) Calcium transport pathways in the nucleus. *Pflugers Arch* **432**, 1–6.
- 58 Martelli AM, Mazzotti G & Capitani S (2004) Nuclear protein kinase C isoforms and apoptosis. *Eur J Histochem* **48**, 89–94.
- 59 Petersen OH, Gerasimenko OV, Gerasimenko JV, Mogami H & Tepikin AV (1998) The calcium store in the nuclear envelope. *Cell Calcium* **23**, 87–90.
- 60 Pan S, Sharma P, Shah SD & Deshpande DA (2017) Bitter taste receptor agonists alter mitochondrial function and induce autophagy in airway smooth muscle cells. *Am J Physiol Lung Cell Mol Physiol* **313**, L154–L165.
- 61 Salvestrini V, Ciciarello M, Pensato V, Simonetti G, Laginestra MA, Bruno S, Pazzaglia M, De Marchi E, Forte D, Orecchioni S *et al.* (2020) Denatonium as a bitter taste receptor agonist modifies transcriptomic profile and functions of acute myeloid leukemia cells. *Front Oncol* **10**, 1225.
- 62 Sharma P, Panebra A, Pera T, Tiegs BC, Hershfeld A, Kenyon LC & Deshpande DA (2016) Antimitogenic effect of bitter taste receptor agonists on airway smooth muscle cells. *Am J Physiol Lung Cell Mol Physiol* **310**, L365–376.
- 63 Wen X, Zhou J, Zhang D, Li J, Wang Q, Feng N, Zhu H, Song Y, Li H & Bai C (2015) Denatonium inhibits growth and induces apoptosis of airway epithelial cells through mitochondrial signaling pathways. *Respir Res* **16**, 13.
- 64 Singh N, Shaik FA, Myal Y & Chelikani P (2020) Chemosensory bitter taste receptors T2R4 and T2R14 activation attenuates proliferation and migration of breast cancer cells. *Mol Cell Biochem* **465**, 199–214.
- 65 Martin LTP, Nachtigal MW, Selman T, Nguyen E, Salsman J, Delleire G & Dupre DJ (2019) Bitter taste receptors are expressed in human epithelial ovarian and prostate cancers cells and nospapine stimulation impacts cell survival. *Mol Cell Biochem* **454**, 203–214.
- 66 Kim UK, Jorgenson E, Coon H, Leppert M, Risch N & Drayna D (2003) Positional cloning of the human quantitative trait locus underlying taste sensitivity to phenylthiocarbamide. *Science* **299**, 1221–1225.
- 67 Risso D, Tofanelli S, Morini G, Luiselli D & Drayna D (2014) Genetic variation in taste receptor pseudogenes provides evidence for a dynamic role in human evolution. *BMC Evol Biol* **14**, 198.
- 68 An Y, Holsinger FC & Husain ZA (2016) De-intensification of adjuvant therapy in human papillomavirus-associated oropharyngeal cancer. *Cancers Head Neck* **1**, 18.
- 69 Swisher-McClure S, Lukens JN, Aggarwal C, Ahn P, Basu D, Bauml JM, Brody R, Chalian A, Cohen RB, Fotouhi-Ghiam A *et al.* (2020) A phase 2 trial of alternative volumes of oropharyngeal irradiation for de-intensification (AVOID): omission of the resected primary tumor bed after transoral robotic surgery for human papilloma virus-related squamous cell carcinoma of the oropharynx. *Int J Radiat Oncol Biol Phys* **106**, 725–732.
- 70 Schwarzer C, Fu Z, Patanwala M, Hum L, Lopez-Guzman M, Illek B, Kong W, Lynch SV & Machen TE (2012) *Pseudomonas aeruginosa* biofilm-associated homoserine lactone C12 rapidly activates apoptosis in airway epithelia. *Cell Microbiol* **14**, 698–709.
- 71 Schwarzer C, Fu Z, Shuai S, Babbar S, Zhao G, Li C & Machen TE (2014) *Pseudomonas aeruginosa* homoserine lactone triggers apoptosis and Bak/Bax-independent release of mitochondrial cytochrome C in fibroblasts. *Cell Microbiol* **16**, 1094–1104.
- 72 Pearson JP, Gray KM, Passador L, Tucker KD, Eberhard A, Iglewski BH & Greenberg EP (1994) Structure of the autoinducer required for expression of *Pseudomonas aeruginosa* virulence genes. *Proc Natl Acad Sci USA* **91**, 197–201.
- 73 Banerjee S, Tian T, Wei Z, Peck KN, Shih N, Chalian AA, O'Malley BW, Weinstein GS, Feldman MD, Alwine J *et al.* (2017) Microbial signatures associated with oropharyngeal and oral squamous cell carcinomas. *Sci Rep* **7**, 4036.
- 74 Carey RM, Rajasekaran K, Seckar T, Lin X, Wei Z, Tong CCL, Ranasinghe VJ, Newman JG, O'Malley BW Jr, Weinstein GS *et al.* (2020) The virome of HPV-positive tonsil squamous cell carcinoma and neck metastasis. *Oncotarget* **11**, 282–293.
- 75 Pushalkar S, Ji X, Li Y, Estilo C, Yegnanarayana R, Singh B, Li X & Saxena D (2012) Comparison of oral

- microbiota in tumor and non-tumor tissues of patients with oral squamous cell carcinoma. *BMC Microbiol* **12**, 144.
- 76 Rajasekaran K, Carey RM, Lin X, Seckar TD, Wei Z, Chorath K, Newman JG, O'Malley BW, Weinstein GS, Feldman MD *et al.* (2021) The microbiome of HPV-positive tonsil squamous cell carcinoma and neck metastasis. *Oral Oncol* **117**, 105305.
- 77 Schmidt BL, Kuczynski J, Bhattacharya A, Huey B, Corby PM, Queiroz EL, Nightingale K, Kerr AR, DeLacure MD, Veeramachaneni R *et al.* (2014) Changes in abundance of oral microbiota associated with oral cancer. *PLoS One* **9**, e98741.
- 78 Gopalakrishnan V, Helmink BA, Spencer CN, Reuben A & Wargo JA (2018) The influence of the gut microbiome on cancer, immunity, and cancer immunotherapy. *Cancer Cell* **33**, 570–580.
- 79 Zitvogel L, Ma Y, Raoult D, Kroemer G & Gajewski TF (2018) The microbiome in cancer immunotherapy: diagnostic tools and therapeutic strategies. *Science* **359**, 1366–1370.
- Fig. S4.** Bitter (T2R) agonists activate calcium responses in HNSCC cell line.
- Fig. S5.** Bitter (T2R) agonists activate calcium responses in HNSCC.
- Fig. S6.** Pharmacology of the Ca^{2+}_i response.
- Fig. S7.** Inhibition of denatonium-induced fluo-4 Ca^{2+} responses with knockdown of T2R4.
- Fig. S8.** Inhibition of denatonium-induced or flufenamic acid (FFA)-induced R-GECO-nls Ca^{2+}_{nuc} responses with TAS2R4 or TAS2R14 shRNA, respectively.
- Fig. S9.** Reduced Ca^{2+}_{nuc} responses in primary oral keratinocytes compared with HNSCC cells.
- Fig. S10.** Nuclear Ca^{2+} responses appeared to propagate to mitochondria in Fluo-8-loaded cells.
- Fig. S11.** Inhibition of denatonium-induced TMRE, JC-1, and CellEvent changes by GPCR inhibitors.
- Fig. S12.** Lack of effect of T2R stimulation on TMRE, JC-1, and CellEvent fluorescence in primary keratinocytes.
- Fig. S13.** Confirmation of caspase activation by Flip-GFP and dependence of denatonium-induced caspase activation on Ca^{2+} signaling.
- Fig. S14.** Flip-GFP measurement of caspase activation in response to denatonium benzoate but not sodium benzoate in SCC4, SCC47, SCC90, and SCC152.
- Fig. S15.** Confirmation of bitter agonist-induced caspase activation by ratiometric caspase biosensor.
- Fig. S16.** Confirmation of denatonium-induced caspase activation by Western for caspase 3 and 7 cleavage in SCC47 cells.
- Fig. S17.** Disease-free survival for TAS2R expression alterations in HNSCC.
- Fig. S18.** TAS2R genomic and expression alterations are prevalent in HNSCC.

Supporting information

Additional supporting information may be found online in the Supporting Information section at the end of the article.

Table S1. Catalogue numbers for key biological and chemical reagents used in this study.

Table S2. Clinical data for HNSCC patients.

Fig. S1. Variable mRNA expression of bitter (T2R) taste receptor genes in HNSCC cell lines.

Fig. S2. Confirmation of endogenous T2R protein expression by Western blot.

Fig. S3. T2Rs are expressed in HNSCC cell lines.